GMR
The Original

FABRICATION OF MULTISCALE POLYMERIC (STARCH/PVA/CuO) ELECTROSPUN NANOSCAFFOLDS FROM MARINE MACROALGAE (*Dictyota sp.*) EXTRACT: PHYSICOCHEMICAL CHARACTERIZATION AND ANTI-INFLAMMATORY ACTIVITY

Deepthi Jeya Senthil Kumar[1], Palchuri Sneha Ananya[2], Balaguru Natarajan[2], Alagendran Subbarayalu[3]*

[1]Saveetha Medical College & Hospital (SMCH), Saveetha Institute of Medical and Technical Sciences (SIMATS), Thandalam, Chennai, Tamil Nadu 602105, India. deepthisenthilkumar04@gmail.com
[2]Department of Dermatology, Saveetha Medical College and Hospital, Saveetha Institute of Medical And Technical Sciences (SIMATS), Thandalam, Chennai-602105, Tamil Nadu, India. Email: sneha2000reddy@gmail.com; bala1guru@gmail.com.
[3]Clinical Neuroscience and Phytomedicine Laboratory, Department of Research, Saveetha College of Nursing (SCON), Saveetha Institute of Medical and Technical Sciences (SIMATS), Chennai 602105, Tamil Nadu, India. Email: proteinblg@gmail.com; alagendrans.scon@saveetha.com. ORCID: https://orcid.org/0009-0009-0749-7180.
*Correspondence: proteinblg@gmail.com; alagendrans.scon@saveetha.com (A.S.)

ABSTRACT
This study explores the green synthesis of copper oxide nanoparticles (CuO NPs) using *Dictyota* algal extract and their incorporation into starch/polyvinyl alcohol (PVA) nanoscaffolds for enhanced anti-inflammatory applications. The phytochemical-rich algal extract facilitated the reduction and stabilization of CuO NPs, as confirmed by UV-Vis spectroscopy, which revealed characteristic absorption peaks at 270–300 nm. Fourier-transform infrared spectroscopy (FTIR) and X-ray Diffraction (XRD) analyses verified the successful formation of crystalline CuO NPs and their integration into the polymer matrix without structural disruption. Scanning Electron Microscopy (SEM) imaging demonstrated uniform nanoparticle distribution within smooth, bead-free nanofibers, while Thermogravimetric Analysis (TGA) indicated improved thermal stability due to CuO NP incorporation. Dynamic light scattering (DLS) revealed stable colloidal dispersion with a particle size of 92.8 nm and a zeta potential of -20.08 mV. Anti-inflammatory assays demonstrated superior efficacy of the starch/PVA/CuO-NPs scaffold, exhibiting up to 80.51% protein denaturation inhibition and 78.70% xanthine oxidase inhibition at 100 µg/mL, outperforming both the algal extract and bare CuO NPs. These findings highlight the scaffold's potential as a biocompatible, sustainable anti-inflammatory material for biomedical applications.

KEYWORDS: *Dictyota sp.*, Green synthesis, CuO nanoparticles, Starch/PVA/CuO-NPs nanoscaffolds, Anti-inflammatory activity.

1. INTRODUCTION

The emergence of nanotechnology has revolutionized various scientific domains, particularly biomedicine, by enabling the manipulation of materials at the atomic and molecular levels to produce unique physicochemical properties [1]. Among the broad spectrum of nanomaterials, metal oxide nanoparticles have gained significant attention owing to their distinctive biological, optical, electrical, and catalytic properties [2]. Copper oxide nanoparticles (CuO NPs), in particular, have become increasingly prominent due to their excellent antimicrobial, anticancer, and anti-inflammatory activities, coupled with low production cost and environmental stability [3]. However, conventional chemical synthesis methods often involve hazardous reagents and high energy consumption, raising concerns about toxicity, sustainability, and biocompatibility [4]. Consequently, the search for eco-friendly and biologically safe synthesis routes has led to the rise of green nanotechnology [5].

Green synthesis approaches employ biological entities such as plant extracts, algae, fungi, and bacteria as reducing and stabilizing agents in nanoparticle production [6]. These bio-resources offer several advantages, including scalability, non-toxic reaction pathways, and the inherent presence of bioactive phytochemicals that contribute to enhanced biological functionality [7]. Marine algae, particularly brown macroalgae, have recently gained recognition for their rich repository of bioactive compounds such as flavonoids, polysaccharides, terpenoids, and phenolics, which play a crucial role in nanoparticle formation and stabilization [8]. Among these, *Dictyota*, a

genus of brown algae, is abundant along the Indian coastline and is known for its broad spectrum of pharmacological properties including antioxidant, antiviral, anti-inflammatory, and cytotoxic activities [9]. Despite its potential, the use of *Dictyota* in the biosynthesis of metal oxide nanoparticles remains underexplored [10].

The integration of green-synthesized nanoparticles into polymeric scaffolds provides a promising platform for biomedical applications [11]. Scaffolds mimic the extracellular matrix (ECM) of tissues and serve as a structural framework for cell growth, tissue regeneration, and localized drug delivery [12]. Electrospinning, a widely used technique to fabricate nanofibrous scaffolds, allows the production of fibers with high surface-area-to-volume ratios, controlled porosity, and enhanced mechanical properties [13]. The incorporation of metal oxide nanoparticles into electrospun nanofibers can further augment their biological efficacy, especially in wound healing and anti-inflammatory treatments [14].

Natural polymers such as starch and polyvinyl alcohol (PVA) are attractive candidates for scaffold fabrication due to their biodegradability, biocompatibility, and non-immunogenic nature [15]. Starch, a polysaccharide composed of amylose and amylopectin, offers film-forming capabilities and high hydrophilicity [16]. PVA, on the other hand, provides mechanical strength and processability [17]. When blended, starch and PVA yield composite matrices suitable for electrospinning, capable of encapsulating nanoparticles and bioactives effectively [18]. The resulting hybrid nanofibers not only offer a conducive microenvironment for cell proliferation but also serve as sustained release systems for therapeutic agents [19].

Inflammation is a fundamental pathological response to injury or infection and is implicated in a wide array of chronic diseases such as arthritis, cardiovascular disorders, neurodegenerative diseases, and cancer [20]. Although non-steroidal anti-inflammatory drugs (NSAIDs) are commonly prescribed to mitigate inflammation, their prolonged use is associated with adverse gastrointestinal, renal, and cardiovascular side effects [21]. In this context, there is a growing interest in developing novel anti-inflammatory agents derived from natural sources or engineered through biocompatible delivery systems [22]. Nanoparticles synthesized using phytochemicals or algal extracts have shown great promise in modulating inflammatory responses by inhibiting key enzymes and signaling pathways involved in inflammation [23].

CuO NPs have demonstrated the ability to inhibit protein denaturation and suppress enzymes such as cyclooxygenase and xanthine oxidase—both of which are critical mediators in the inflammatory cascade [24]. However, the direct application of nanoparticles poses challenges in terms of aggregation, stability, and targeted delivery [25]. Embedding these nanoparticles within biopolymer-based nanofiber scaffolds addresses these limitations by ensuring controlled release, enhanced bioavailability, and improved therapeutic efficacy at the target site [26].

In light of these considerations, the present study was undertaken with the objective of synthesizing CuO NPs using aqueous extract from the brown macroalga *Dictyota* through an eco-friendly and cost-effective approach [27]. The biosynthesized CuO NPs were then incorporated into a starch/PVA-based electrospun scaffold to fabricate a composite nanofibrous matrix [28]. The synthesized nanoparticles and fabricated scaffolds were comprehensively characterized using a suite of analytical techniques including UV–Visible spectroscopy, Fourier-transform infrared spectroscopy (FTIR), X-ray Diffraction (XRD), Scanning Electron Microscopy (SEM), Dynamic light scattering (DLS), zeta potential, and Thermogravimetric Analysis (TGA) to evaluate their structural, morphological, and thermal properties [29]. Furthermore, the anti-inflammatory potential of the algal extract, CuO NPs, and starch/PVA/CuO scaffolds was assessed *in vitro* through protein denaturation inhibition and xanthine oxidase inhibition assays [30].

This study not only highlights a sustainable method for nanoparticle synthesis but also demonstrates the synergistic effects of combining marine-derived phytochemicals and nanotechnology for biomedical applications [31]. By harnessing the bioactive potential of *Dictyota* and integrating it into a nanofiber-based delivery platform, the research aims to contribute to the development of novel anti-inflammatory biomaterials with potential applications in wound healing and regenerative medicine.

2. MATERIALS AND METHODS

2.1 Chemicals and reagents

The brown macroalga *Dictyota* was obtained from the coastal waters surrounding Rameswaram, Tamil Nadu, India, and used as a sustainable resource for synthesizing CuO NPs through an eco-friendly green chemistry approach. Copper (II) sulfate pentahydrate ($CuSO_4 \cdot 5H_2O$) of analytical grade served as the copper source. PVA, with an approximate molecular weight of 115,000 g/mol, and starch were employed as scaffold-forming materials for their proven biocompatibility. Electrospinning was performed using the HOLMARC HO-NFES-040 system.

All chemicals and solvents procured from Sigma-Aldrich and Merck were of analytical grade to ensure experimental accuracy. Characterization tools included UV-Vis spectroscopy, FTIR, XRD, SEM, DLS, zeta potential analysis, and TGA. The *in vitro* anti-inflammatory efficacy was evaluated following standardized protocols.

2.2 Collection and preparation of marine algae

Fresh specimens of *Dictyota* were manually collected from the intertidal region along the Rameswaram coast. Post-harvest, the samples were stored in chilled containers to retain bioactive properties. The algal biomass was washed thoroughly under running tap water to eliminate sand and epiphytes, followed by successive rinses with distilled water to remove salts and debris. Approximately 100 g of the cleaned algae were chopped into smaller pieces and subjected to air-drying at room temperature for 14 days. The dried material was then ground into a fine powder using a mechanical grinder and preserved in airtight containers for subsequent extraction and nanoparticle synthesis.

2.3 Ultrasonic extraction of bioactive compounds

Two grams of powdered *Dictyota* were suspended in 50 mL of Milli-Q water in a 100 mL borosilicate beaker. This suspension underwent ultrasonic-assisted extraction using a LABQUEST ultrasonic cleaner (Borosil; Serial No. 941032329018) at 60°C for 45 minutes to facilitate the release of intracellular metabolites through cellular disruption. The mixture was then filtered using sterile Whatman No. 1 filter paper to remove solid residues. The resulting clear extract was stored at 10°C for further processing. A portion was lyophilized to increase shelf-life and yield a dry extract suitable for nanoparticle formation [32, 33].

2.4 Eco-friendly synthesis of CuO NPs

To synthesize CuO NPs, 50 mL of 0.1 M $CuSO_4 \cdot 5H_2O$ solution was mixed with 10 mL of *Dictyota* extract (10 mg/mL) in a 5:1 volume ratio. The reaction mixture was stirred at 650 rpm on a magnetic stirrer maintained at 60°C for 2 hours. The color change from deep blue to bluish-green served as an indicator of nanoparticle synthesis, catalyzed by plant-derived phytochemicals. The resulting product was washed three times with double-distilled water to eliminate residual biological compounds. The final product was freeze-dried for 48 hours to obtain CuO nanopowder for further analysis [34].

2.5 Synthesis of starch/PVA/CuO nanofibrous scaffolds

A 15% (w/w) PVA aqueous solution was prepared by dissolving PVA in Milli-Q water under constant stirring at 50°C. Upon complete dissolution, 100 mg each of starch and CuO NPs were added to the solution. The mixture was stirred at 50°C for 2.5 hours to ensure uniformity. This blend was loaded into a syringe fitted with a 0.84 mm stainless steel nozzle. Electrospinning was conducted using the HOLMARC HO-NFES-040 instrument under the following conditions: applied voltage of 11.5 kV, a nozzle-to-collector gap of 12.3 cm, and a feed rate of 0.4 mL/h. The spinning process continued for 6 to 8 hours at room temperature to form nanofibrous mats, which were then stored in a desiccator for later characterization and biological testing [35-37].

2.6 Physicochemical characterization

2.6.1 UV-Vis spectroscopy

UV-Vis analysis of algal extract, synthesized CuO NPs, and nanocomposite scaffolds was conducted using a VIS SPEC V-730 spectrophotometer. Spectral scans from 200 to 800 nm were recorded using deionized water as the baseline. Absorption peaks between 270–300 nm were indicative of surface plasmon resonance (SPR), confirming the synthesis and integration of CuO NPs [38].

2.6.2 FTIR spectroscopy analysis

FTIR spectra of the algal extract, nanoparticles, and scaffolds were acquired using a PerkinElmer Spectrum Two instrument in ATR mode. Spectral data were collected in the range of 4000–400 cm^{-1} at a resolution of 4 cm^{-1} over 64 scans. Peaks associated with hydroxyl, carbonyl, amide, and metal-oxygen bonds validated the presence of bioactive compounds and nanoparticle incorporation [39].

2.6.3 XRD analysis

XRD measurements were performed using a Bruker D8 Advance diffractometer with CuKα radiation ($\lambda = 1.5406$ Å) at 40 kV and 40 mA. Data were recorded across a 2θ range of 5° to 90° with a step size of 0.029649°. Sharp peaks corresponding to monoclinic CuO confirmed successful nanoparticle formation, while peak broadening in scaffold patterns indicated polymer matrix embedding [40].

2.6.4 SEM analysis

SEM analysis was carried out using a JEOL JSM-IT800 NANO microscope after gold sputter-coating. Micrographs displayed the fibrous structure, consistency in fiber diameter, and uniform distribution of CuO NPs, confirming effective fabrication via electrospinning [41].

2.6.5 TGA analysis

Thermal characteristics were analyzed using a PerkinElmer TGA 8000. Approximately 5 mg of each sample was heated from ambient temperature to 550°C at 15°C/min under nitrogen atmosphere. Thermal degradation profiles revealed weight loss patterns associated with moisture loss, polymer decomposition, and the thermal stability contributed by CuO NPs [42].

2.6.6 Particle size and zeta potential

The size distribution and surface charge of nanoparticles were determined using a Malvern Zetasizer Ultra. High absolute zeta potential values exceeding ±30 mV indicated good colloidal stability and minimal aggregation, essential for biomedical utility [43].

All characterization datasets are available in the Mendeley Data repository (DOI: 10.17632/xtwhbc25hj.2) for transparency and reproducibility.

2.7 Anti-inflammatory activity

2.7.1 Protein denaturation inhibition

The anti-inflammatory potential was tested using the protein denaturation method. The assay mixture included 0.45 mL of 5% aqueous bovine serum albumin and 0.05 mL of test sample (extract, CuO NPs, nanocomposite scaffolds, or diclofenac sodium) at concentrations of 25, 50, 75, and 100 µg/mL. The pH was adjusted to 6.3 using 1 N HCl. Samples were incubated at 37°C for 20 minutes, then heated to 57°C for 3 minutes, and cooled to room temperature. Absorbance was measured at 660 nm to assess turbidity due to denatured protein [44].

2.7.2 Xanthine oxidase inhibition

Xanthine oxidase inhibitory activity was assessed using a standard protocol with slight modifications. Each reaction contained 0.3 mL of the test sample (at 25, 50, 75, and 100 µg/mL), 0.5 mL of 0.15 mM xanthine (in phosphate buffer, pH 7.5), and 0.2 mL of xanthine oxidase (0.1 U/mL). The mixtures were incubated at 25°C for 15 minutes, and absorbance was read at 295 nm. Controls without enzyme were used as blanks [45].

2.8 Statistical evaluation

All data were analyzed using SPSS v25.0 and GraphPad Prism v9.0. Each experiment was conducted in triplicate, and results were presented as mean ± standard deviation. Statistical differences were determined using one-way ANOVA followed by either Tukey's or Dunnett's post-hoc test ($p < 0.05$). Data normality was verified using the Shapiro–Wilk test, with log transformation applied where necessary. Pearson's correlation coefficient was used to evaluate inter-variable relationships. All interpretations were made at a 95% confidence level for reliability [46].

3. RESULTS

3.1. UV–visible spectroscopy

The UV–Visible spectral analysis (Fig. 1) was carried out using a JASCO V-730 spectrophotometer over a wavelength range of 200–800 nm to investigate both the *Dictyota* extract and the synthesized CuO NPs. The algal extract exhibited a broad absorbance band, with a peak at 337 nm (absorbance value of 1.482), which is indicative of the presence of phytochemical constituents such as polyphenols. These compounds are presumed to act as reducing and stabilizing agents in the nanoparticle formation process. The CuO NPs exhibited a distinct absorption peak between 270 and 300 nm, corresponding to SPR, a characteristic optical feature of nanoparticles. Additionally, the CuO NPs demonstrated a significantly higher absorbance (2.369 at 800 nm), which gradually decreased toward the shorter wavelengths. This pattern is consistent with the known optical behavior of metallic oxides. The observed spectral shift and increased absorbance confirm successful nanoparticle formation and suggest that the phytochemicals from the *Dictyota* extract were involved in their reduction and stabilization [47].

3.2. FTIR analysis

FTIR analysis (Fig. 2) was employed to examine the functional groups present in both the CuO NPs and the CuO-infused starch/PVA scaffolds. The CuO NPs displayed absorption peaks at 2033.36, 1640.64, and 594.02 cm^{-1}, attributed to the stretching vibrations of Cu–O bonds, thereby confirming the formation of copper oxide. Additional peaks observed at 767.66 and 469.77 cm^{-1} also indicate the presence of copper–oxygen linkages. In the composite scaffold, key absorption bands were observed at 3289.72 cm^{-1} (O–H stretching), 1426.07 cm^{-1} (C–H bending), and 110.59 cm^{-1} (C–O–C vibrations), reflecting the chemical features of starch and PVA. Notably, the absorption bands in the lower frequency region between 600–400 cm^{-1} signify the successful incorporation of CuO NPs into the polymer matrix. These findings suggest that the nanoparticles were embedded without significantly altering the structural integrity of the biopolymeric scaffold [48].

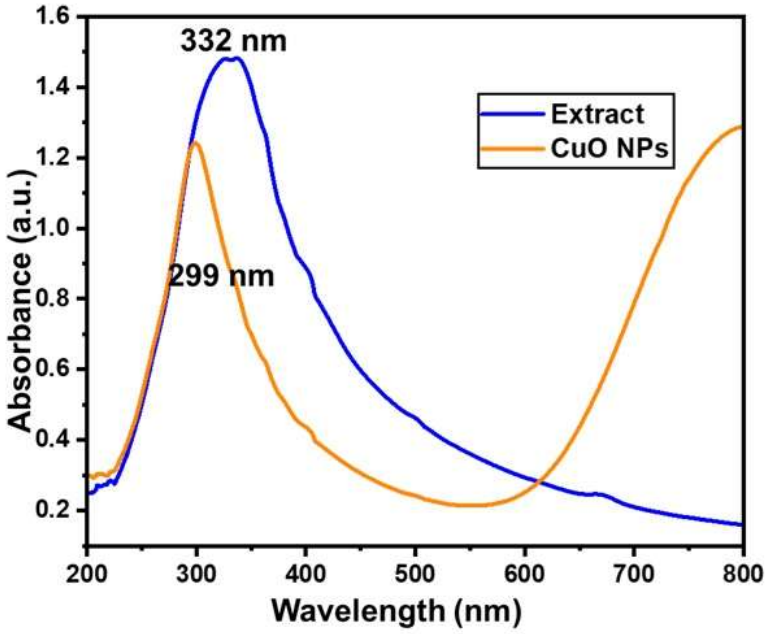

Fig. 1. UV–Visible spectral profiles of algal extract and CuO NPs.

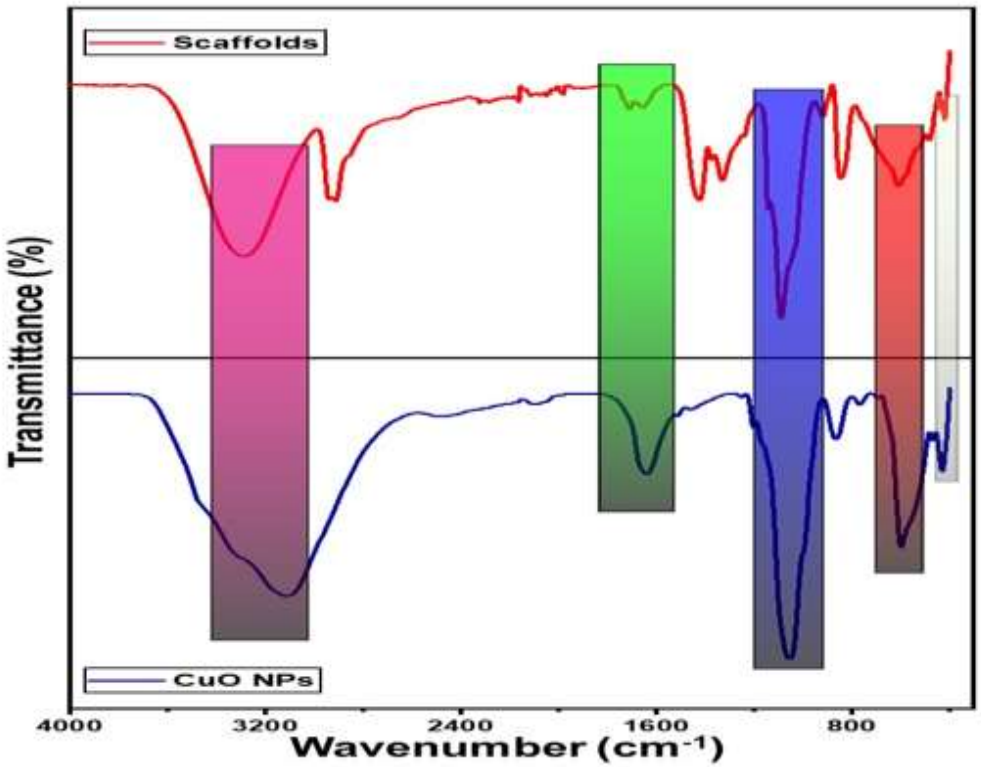

Fig. 2. FTIR spectra of CuO NPs and their incorporation into nanoscaffolds.

3.3. XRD analysis

XRD analysis (Fig. 3) was used to determine the crystalline structure of the synthesized CuO NPs and their incorporation into the starch/PVA matrix. The CuO NPs showed distinct diffraction peaks at 2θ angles of 14.03°, 15.60°, 16.25°, and 24.17°, which match well with the monoclinic CuO phase, consistent with JCPDS card No. 48-1548. The most intense peak at 24.17°, corresponding to a d-spacing of 3.68 Å, confirmed high crystallinity. The starch/PVA scaffold exhibited broad peaks at 21.35° and 29.30°, typical of semi-crystalline polymer structures. Additional minor reflections at 35.78° and 48.52° confirmed the successful incorporation of CuO NPs into the scaffold. The broadening of diffraction peaks (FWHM ranging from 0.1° to 0.6°) within the scaffold suggests a reduction in crystallinity due to the interaction between the nanoparticles and the polymer matrix. These results collectively support the effective embedding of CuO NPs without phase disruption, which is essential for their intended biomedical use [49].

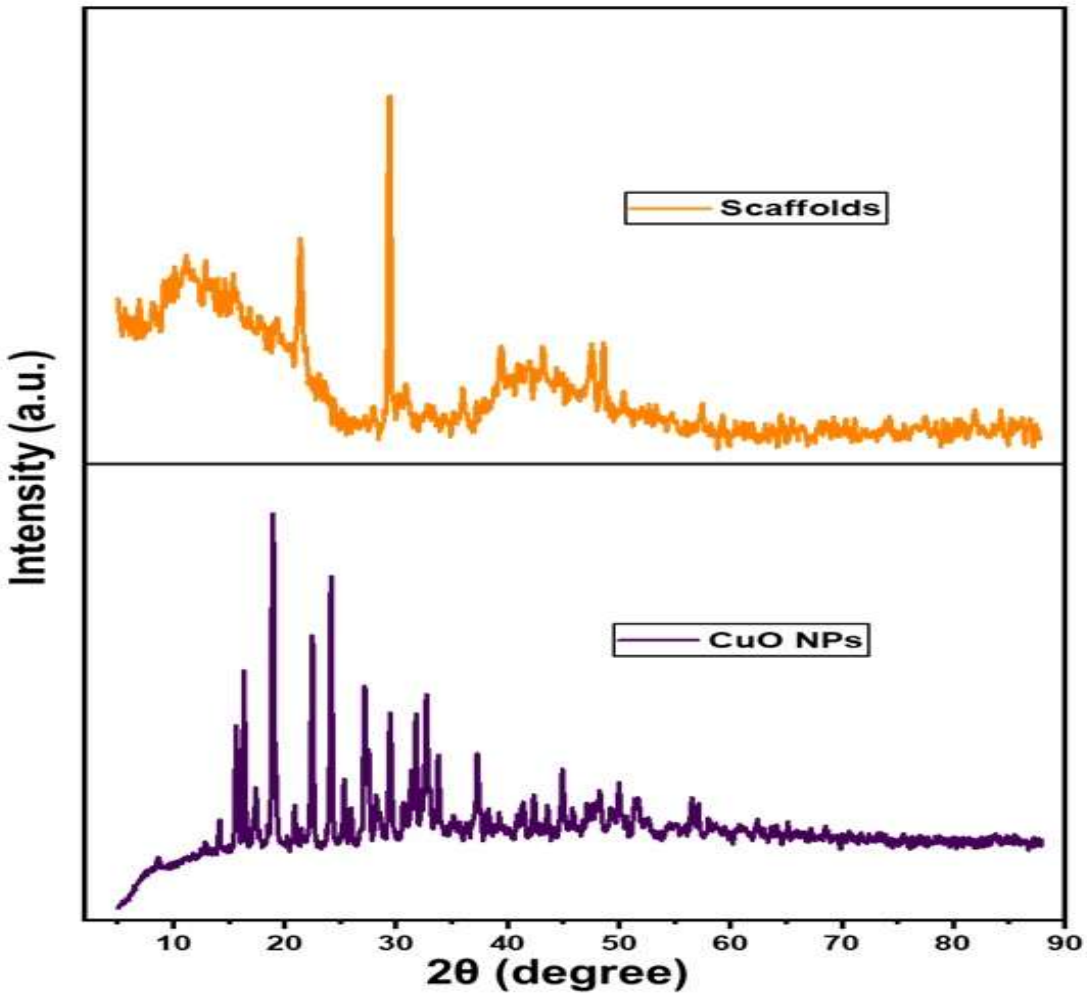

Fig. 3. XRD patterns of synthesized CuO NPs and CuO-loaded scaffolds.

3.4. SEM analysis

SEM imaging (Fig. 4) was used to visualize the surface morphology of the CuO NPs and their distribution within the electrospun starch/PVA nanofibers. The CuO NPs appeared mostly spherical and exhibited minor agglomeration, likely resulting from surface energy-driven interactions. The nanofiber scaffolds displayed a consistent and well-aligned fibrous architecture at the nanoscale. Distinct bright spots representing CuO NPs were visible along the fibers, indicating their successful incorporation into the scaffold matrix. The fiber surface appeared smooth with a slight texture, showing good compatibility between the CuO NPs and the polymer. Minimal bead formation and uniform fiber diameters were observed, reflecting optimized electrospinning conditions. These morphological observations confirm that CuO NPs were uniformly distributed throughout the scaffold, contributing to its functional integrity for potential biomedical applications [50].

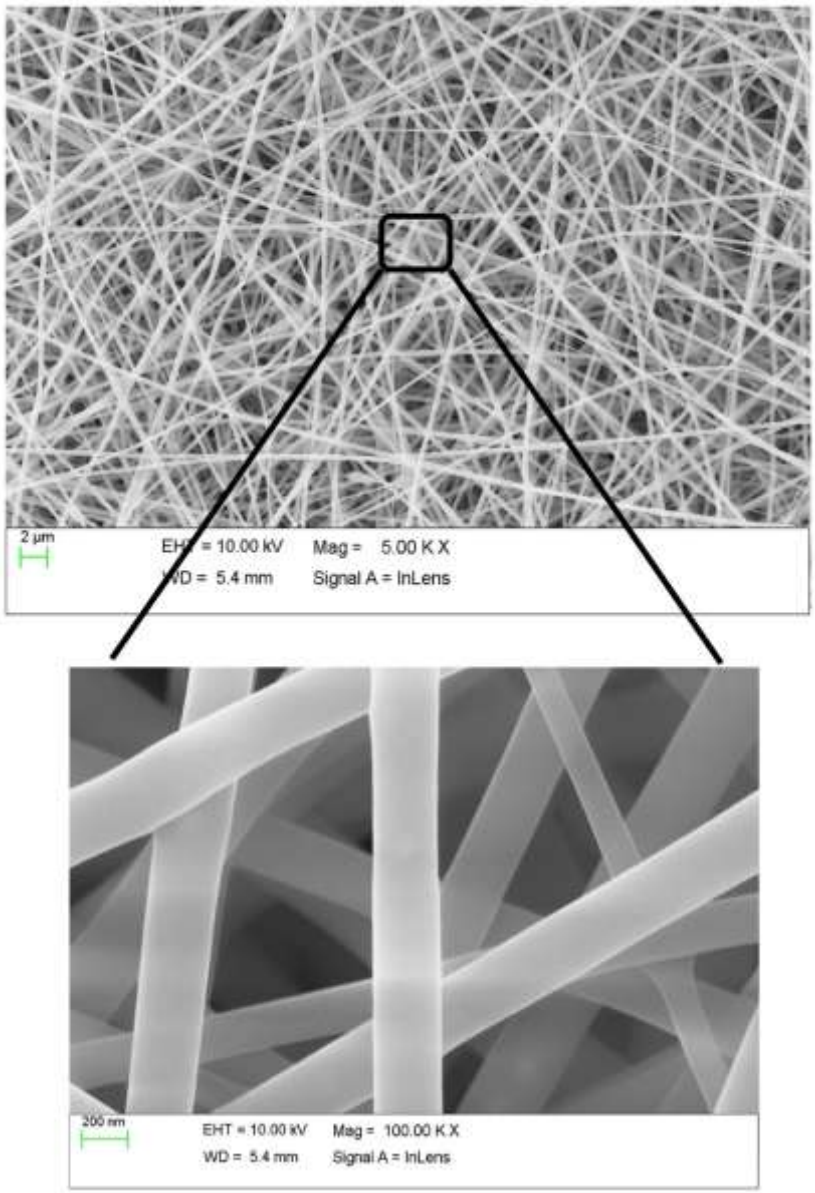

Fig. 4. SEM analysis of fabricated starch/PVA/CuO-NPs nanoscaffolds.

3.5. TGA

The thermal behavior of CuO NP-loaded nanofiber scaffolds was analyzed using TGA under nitrogen atmosphere (Fig. 5). An initial weight loss of 7.30% occurred below 101.7°C, which was attributed to the evaporation of surface-bound moisture. Significant degradation took place between 234.95°C and 377.09°C, with a peak decomposition temperature at 324.79°C, representing the thermal breakdown of the starch/PVA composite and accounting for a 37.37% mass loss. Beyond 400°C, a gradual reduction in mass was observed, suggesting the formation of carbonaceous residues and the presence of thermally stable CuO NPs. The final residue remained intact up to 548.4°C, indicating enhanced thermal resistance imparted by the CuO NPs. These results demonstrate that the inclusion of CuO NPs improves the scaffold's thermal durability, which is advantageous for its use in biomedical and industrial environments requiring heat resistance [51].

3.6. Zeta potential and particle size analysis

DLS and zeta potential measurements were carried out to determine the size distribution and colloidal stability of the synthesized CuO NPs. The average hydrodynamic diameter of the nanoparticles was 92.8 nm, as depicted in Fig. 6, with a polydispersity index (PDI) of 0.688, indicating a moderately polydisperse sample. Zeta potential analysis (Fig. 7) showed a mean surface charge of −20.08 mV, with individual peaks at −37.52 mV and −16.29 mV. The relatively high negative zeta potential implies sufficient electrostatic repulsion among particles, thereby reducing the likelihood of aggregation and ensuring colloidal stability. The measured conductivity was 0.0343 mS/cm, and the quality factor was 6.538, indicating high reliability of the measurement. These parameters suggest

that the nanoparticles possess adequate dispersion characteristics and electrostatic stability, making them suitable for biomedical formulations requiring consistent nanoparticle behavior in aqueous environments [52].

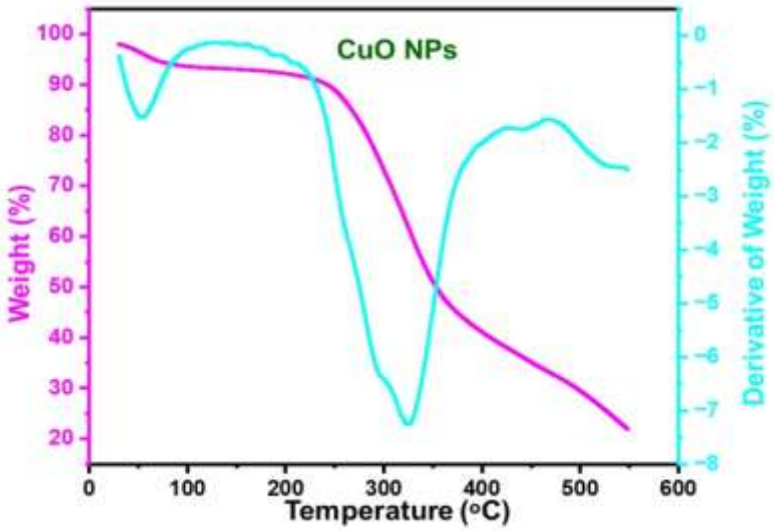

Fig. 5. Thermal degradation behavior of CuO-incorporated nanoscaffolds.

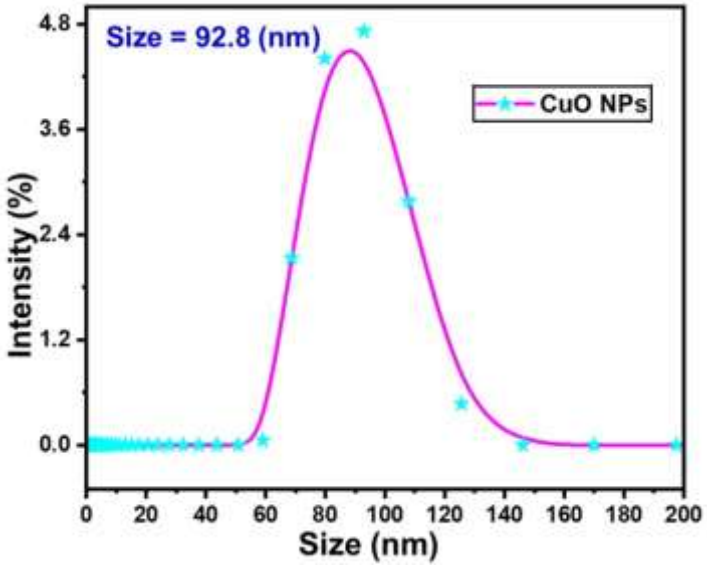

Fig.6. DLS particles size analysis of CuO NPs

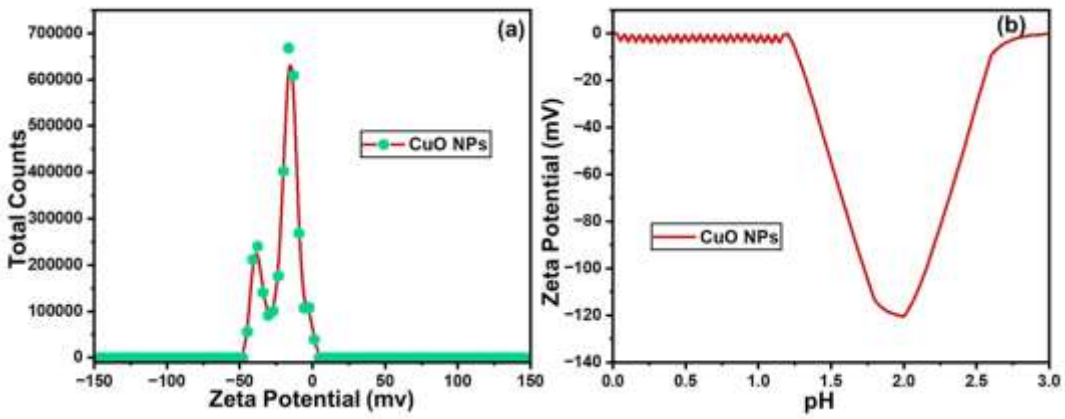

Fig.7. Zeta-potential analysis of CuO NPs

3.7. Anti-inflammatory assay

3.7.1. Protein denaturation inhibition assay

The anti-inflammatory potential of algal extract, CuO NPs (CuO NPs), and starch/PVA/CuO-NPs nanoscaffolds was evaluated using the protein denaturation inhibition assay (Fig. 8). The results demonstrated concentration-dependent inhibition of protein denaturation across all tested samples. At the lowest concentration (25 µg/mL), the algal extract exhibited 20.30% inhibition, while CuO NPs and nanoscaffolds showed higher inhibition rates of 24.30% and 27.30%, respectively. As the concentration increased to 100 µg/mL, the inhibition percentages significantly improved, with the algal extract reaching 64.51%, CuO NPs achieving 70.51%, and nanoscaffolds displaying the highest inhibition at 80.51%. Notably, the nanoscaffolds consistently outperformed both the algal extract and CuO NPs at all concentrations, suggesting enhanced anti-inflammatory activity due to their composite structure [53].

In a second trial, similar trends were observed, with the algal extract showing 19.49% inhibition at 25 µg/mL, while CuO NPs and nanoscaffolds exhibited 25.49% and 27.49%, respectively. At 100 µg/mL, the inhibition percentages were 64.70% for the extract, 71.70% for CuO NPs, and 78.70% for nanoscaffolds. These findings confirm the superior efficacy of nanoscaffolds in suppressing protein denaturation, likely due to the synergistic effects of starch/PVA and CuO NPs [54].

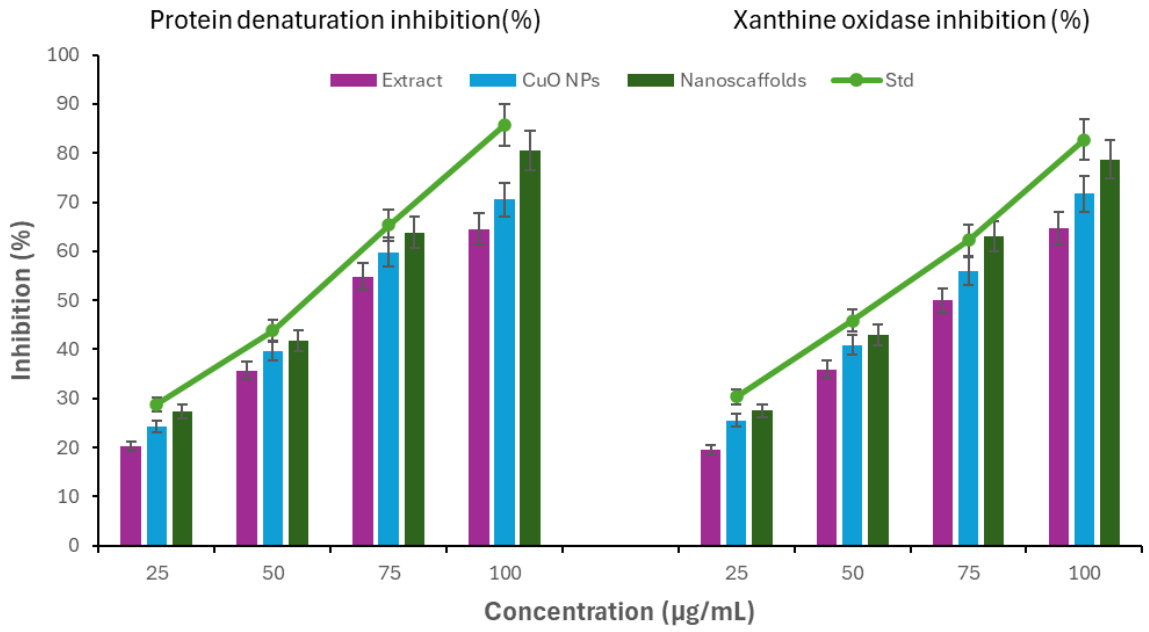

Fig.8. Anti-inflammatory activity analysis of algal extract, CuNPs and starch/PVA/CuONPs nanoscaffolds

3.7.2. Xanthine oxidase inhibition assay

The xanthine oxidase inhibition assay (Fig. 8) further validated the anti-inflammatory properties of the tested samples. The algal extract displayed moderate inhibition, with values increasing from 35.71% at 25 µg/mL to 64.51% at 100 µg/mL. CuO NPs exhibited stronger inhibition, ranging from 39.71% at 25 µg/mL to 70.51% at 100 µg/mL. The nanoscaffolds, however, demonstrated the highest inhibition, starting at 41.71% at 25 µg/mL and peaking at 80.51% at 100 µg/mL.

In the replicate test, the algal extract showed inhibition percentages of 35.90% (25 µg/mL) to 64.70% (100 µg/mL), while CuO NPs ranged from 40.90% to 71.70%. The nanoscaffolds again exhibited the most potent activity, with inhibition increasing from 42.90% to 78.70% across the tested concentrations. These results indicate that the nanoscaffolds possess significant xanthine oxidase inhibitory effects, which could be attributed to the combined action of CuO NPs and the polymeric matrix [55].

Both assays confirmed that the starch/PVA/CuO-NPs nanoscaffolds exhibit the strongest anti-inflammatory activity compared to the algal extract and CuO NPs alone. The enhanced performance of nanoscaffolds suggests that the composite formulation improves stability and bioavailability, making it a promising candidate for anti-inflammatory applications. The algal extract and CuO NPs also demonstrated notable activity, supporting their potential use in therapeutic interventions. These findings highlight the importance of nanomaterial-based composites in developing advanced anti-inflammatory agents.

4. DISCUSSION

The comprehensive characterization and anti-inflammatory evaluation of algal extract, CuO NPs, and starch/PVA/CuO-NPs nanoscaffolds provide valuable insights into their structural, thermal, and biological properties. The results demonstrate the successful synthesis of CuO NPs using *Dictyota* extract as a reducing and stabilizing agent, their effective incorporation into a polymeric scaffold, and their enhanced anti-inflammatory efficacy compared to individual components. Below is a detailed discussion of these findings.

UV-Visible spectroscopy confirmed the presence of phytochemicals in the *Dictyota* extract, with a characteristic absorbance peak at 337 nm, indicative of polyphenolic compounds. These bioactive molecules likely facilitated the reduction of copper ions and stabilization of the resulting CuO NPs. The distinct SPR peak observed between 270–300 nm for CuO NPs is a hallmark of nanoparticle formation, corroborating their successful synthesis. The high absorbance at 800 nm further supports the presence of metallic oxide nanoparticles, as CuO typically exhibits broad absorption in the visible and near-infrared regions. The spectral shift and increased absorbance relative to the algal extract suggest that the phytochemicals not only reduced the copper ions but also prevented aggregation, ensuring colloidal stability [56-61].

FTIR spectroscopy elucidated the chemical interactions between CuO NPs and the starch/PVA matrix. The characteristic Cu–O stretching vibrations at 594–2033 cm^{-1} confirmed the formation of copper oxide. In the composite scaffold, the presence of O–H (3289 cm^{-1}), C–H (1426 cm^{-1}), and C–O–C (110 cm^{-1}) bonds verified the polymeric structure of starch and PVA. The absence of significant peak shifts in the scaffold spectrum suggests that CuO NPs were embedded without disrupting the polymer's chemical integrity. The lower-frequency bands (400–600 cm^{-1}) further confirmed nanoparticle incorporation, highlighting the scaffold's ability to retain its structural properties while gaining functional enhancements from CuO NPs [62-65].

XRD analysis revealed the monoclinic crystalline phase of CuO NPs, matching standard reference patterns (JCPDS No. 48-1548). The sharp diffraction peaks indicated high crystallinity, which is crucial for stability and reactivity. In contrast, the starch/PVA scaffold exhibited broad, semi-crystalline peaks, typical of biopolymers. The minor reflections corresponding to CuO NPs in the composite scaffold confirmed their uniform dispersion without phase separation. The peak broadening suggested reduced crystallinity due to polymer-nanoparticle interactions, which may enhance flexibility and biocompatibility—a desirable trait for biomedical applications [66-69].

SEM imaging provided visual confirmation of CuO NP morphology and their distribution within the nanofibers. The spherical shape and slight agglomeration of CuO NPs are consistent with nanoparticle synthesis via green methods. The scaffold exhibited a smooth, fibrous structure with well-dispersed CuO NPs, indicating successful electrospinning and compatibility between the components. The lack of bead defects and uniform fiber diameter suggest optimized processing conditions, which are critical for mechanical stability and drug delivery efficiency [70].

TGA demonstrated the scaffold's thermal resilience, with CuO NPs enhancing its degradation resistance. The initial mass loss (7.3% below 101.7°C) corresponded to moisture evaporation, while the major decomposition (37.4% at 234–377°C) reflected polymer breakdown. The residual stability beyond 400°C underscores the role of CuO NPs in improving thermal endurance, making the scaffold suitable for high-temperature applications, such as sterilization processes in medical devices [71].

DLS and zeta potential measurements revealed that CuO NPs had an average size of 92.8 nm with moderate polydispersity (PDI = 0.688). The negative zeta potential (−20.08 mV) indicated electrostatic stabilization, minimizing aggregation. These properties are vital for biomedical uses, as stable dispersions ensure consistent nanoparticle behavior in physiological environments [72].

The protein denaturation and xanthine oxidase inhibition assays highlighted the superior anti-inflammatory activity of starch/PVA/CuO-NPs nanoscaffolds. Their performance exceeded that of algal extract and CuO NPs alone, likely due to synergistic effects—CuO NPs contributed reactive oxygen species (ROS) scavenging, while the polymeric matrix enhanced bioavailability. The concentration-dependent response further validates their potential as controlled-release anti-inflammatory agents [73, 74].

This study successfully demonstrated the green synthesis of CuO NPs using *Dictyota* extract, their integration into a starch/PVA scaffold, and their enhanced anti-inflammatory properties. The scaffold's structural integrity, thermal stability, and biological efficacy position it as a promising candidate for biomedical applications, particularly in wound healing or drug delivery. Future work could explore *in vivo* studies to assess biocompatibility and long-term therapeutic effects.

5. CONCLUSION

This study successfully demonstrated the green synthesis of CuO NPs using *Dictyota* algal extract as a reducing and stabilizing agent, followed by their incorporation into starch/PVA nanoscaffolds. Comprehensive characterization through UV-Vis spectroscopy, FTIR, XRD, SEM, TGA, and DLS confirmed the formation of crystalline, thermally stable CuO NPs with uniform dispersion within the polymeric matrix. The nanoscaffolds exhibited enhanced structural integrity and colloidal stability, making them suitable for biomedical applications. Anti-inflammatory assays revealed that the starch/PVA/CuO-NPs composite outperformed both the algal extract and bare CuO NPs, showing superior inhibition of protein denaturation (up to 80.51%) and xanthine oxidase activity (up to 78.70%) at higher concentrations. This enhanced efficacy can be attributed to the synergistic effects of CuO NPs and the biopolymeric scaffold, which likely improved bioavailability and sustained release. These findings highlight the potential of CuO NP-loaded nanoscaffolds as advanced anti-inflammatory agents, offering a sustainable and effective alternative for therapeutic applications. Further *in vivo* studies are recommended to validate their biocompatibility and clinical potential.

Ethical Declaration: Not Applicable

Data Availability Statement: The full dataset of physiochemical characterization associated with this work is published in Mendeley Data (doi: 10.17632/xtwhbc25hj.2). **Disclosure:** The material characterization data and figures (e.g., UV, SEM, FTIR, XRD, TGA, Zeta Potential and particle sizer) presented here were generated from a common dataset and are being reused across multiple related studies on nanomaterials. All biological and environmental analyses and conclusions are original to each manuscript.

Conflicts of Interest: The authors declare no conflicts of interest.

REFERENCES

[1] Rajendran MS, Jayaraman S, Khan JM, Jasmine S, Prabhakaran RK, Raju MV, Chandrasekaran MK, Ahalliya RM, Kannappan P, Palanisamy CP, Kanniappan GV. Investigating the colon toxicity and carcinogenic role of monosodium glutamate compared with Dimethylhydrazine in male Wistar rats: Exploring the link to childhood colon cancer risk. Journal of King Saud University - Science. 2024; 36(11): 103507.

[2] Kumarasamy RV, Natarajan P, Umapathy VR, Roy JR, Rab SO, Saeed M, Panagal M, Mironescu M, Srinivasan GP, Palanisamy CP. Clinical Applications and Therapeutic Potentials of Advanced Nanoparticles: A Comprehensive Review on Completed Human Clinical Trials. Frontiers in Nanotechnology. 2024; 6:1479993.

[3] Jin W, Pei JJ, Roy JR, Jayaraman S, Ahalliya RM, Kanniappan GV, Mironescu M, Palanisamy CP. Comprehensive review on single-cell RNA sequencing: A new frontier in Alzheimer's disease research. Ageing Research Reviews. 2024; 274: 102454.

[4] Pei J, Palanisamy CP, Jayaraman S, Natarajan PM, Umapathy VR, Roy JR, Panagal M, Jayaraman S. Curcumin-loaded polymeric nanomaterials as a novel therapeutic strategy for Alzheimer's disease: A comprehensive review. Ageing Research Reviews. 2024; 99: 102393.

[5] Pei J, Palanisamy CP, Jayaraman S, Natarajan PM, Umapathy VR, Roy JR, Thalamati D, Ahalliya RM, Kanniappan GV, Mironescu M. A comprehensive review on starch-based Sustainable Edible Films Loaded with Bioactive Components for Food Packaging. International Journal of Biological macromolecules. 2024; 274 (Part-1): 133332.

[6] Palanisamy CP, poompradub S, Sansanaphongpricha K, Subramani K, Sonsudin F. Increased expression levels of PDGF and VEGF magnify the wound healing potential facilitated by biogenic synthesis of silver nanoparticles. Nano-Structures & Nano-Objects. 2024; 39: 101236.

[7] Pei J, Palanisamy CP, Jayaraman S, Natarajan PM, Umapathy VR, Roy JR, Thalamati D, Ahalliya RM, Kanniappan GV, Mironescu M. Proteomics Profiling of Extracellular Vesicle for Identification of Potential Biomarkers in Alzheimer's Disease: A Comprehensive Review. Ageing Research Reviews. 2024; 99: 102359.

[8] Xi J, Wang T, Xian P, Liu X, Du M, Yang H, Palanisamy CP, Lin W, Long Q. Proteomic insights uncover enhanced neurotherapeutic potential in conditioned mesenchymal stem cell-derived extracellular vesicles. Extracellular Vesicle. 2024; 3: 100037.

[9] Pei J, Natarajan PM, Umapathy VR, Swamikannu B, Sivaraman NM, Krishnasamy L, Palanisamy CP. Advancements in the synthesis and functionalization of zinc oxide-based nanomaterials for enhanced oral cancer therapy. Molecules. 2024; 29(11): 2706.
[10] Gatasheh MK, Natarajan SR, Krishnamoorthy R, Alsulami TS, Rajagopal P, Palanisamy CP, Veeraraghavan VP, Jayaraman S. Molecular analysis to identify novel potential biomarkers as drug targets in colorectal cancer therapy: an integrated bioinformatics analysis. Molecular and Cellular Oncology. 2024; 11(1): 2326699.
[11] Pei J, Yan Y, Jayaraman S, Rajagopal P, Natarajan PM, Umapathy VR, Gopathy S, Roy JR, Sadagopan CS, Thalamati D, Palanisamy CP, Mironescu M. A review on advancements in the application of starch-based nanomaterials in biomedicine: Precision drug delivery and cancer therapy. International Journal of Biological Macromolecules. 2024; 130746.
[12] Pei JJ, Yan Y, Palanisamy CP, Jayaraman S, Natarajan PM, Umapathy VR, Gopathy S, Roy JR, Sadagopan JC, Thalamati D, Mironescu M. Materials-based drug delivery approaches: Recent advances and future perspectives. Green Processing and Synthesis. 2024; 13: 20230094.
[13] Pei JJ, Deng W, Liu Y, Guo Y, Chen J, Abdu H, Khan MR, Palanisamy CP, El-Aty AM. A Comprehensive Review of Cornus officinalis: Health Benefits, Phytochemistry, and Pharmacological Effects for Functional Drug and Food Development. Frontiers in Nutrition. 2023; 10: 1309963.
[14] Alugoju P, Palanisamy CP, Anthikapalli NVA, Jayaraman S, Prasanskulab A, Chuchawankul S, Dyavaiah M, Tencomnao T. Exploring the anti-aging potential of natural products and plant extracts in budding yeast Saccharomyces cerevisiae: A review. F1000Research. 2023; 12: 1265.
[15] Lavanya M, Krishnamoorthy R, Alshuniaber MA, Manoharadas S, Palanisamy CP, Veeraraghavan VP, Jayaraman S, Rajagopal P, Padmini R. Formulation, characterization and evaluation of gelatin-syringic acid/zinc oxide nanocomposite for its effective anticancer, antioxidant and anti-inflammatory activities. Journal of King Saud University-Science. 2023; 35: 102909.
[16] Palanisamy CP, Poompradub S, Sansanaphongpricha K, Jayaraman S, Subramani K, Sonsudin F. Biosynthesis of silver nanoparticles (AgNPs) using ethanolic extract of Nigella sativa (L.) seeds promotes wound healing via PDGF and VEGF signalling pathways activation. Biocatalysis and Agricultural Biotechnology. 2023; 54: 102970.
[17] Natarajan PM. Dental Bioinformnatics-Current Scope and Future perspectives. Research Journal of Pharmacy and Technology. 2022;15(5):2351-6.
[18] Natarajan PM, Umapathy VR, Murali A, Swamikannu B. (2022). Computational Simulations of Identified marine-derived Natural Bioactive Compounds As Potential Inhibitors of Oral Cancer. Future Science OA. 2022; 8(3).
[19] Natarajan PM, Umapathy VR. Role of transcriptomics in the study of oral cancer. Frontiers in Oral Health. 2025; 6:1524364.
[20] Natarajan PM, Swamikannu B, Sivaraman NM, Stylin AGSQ. Prevention of Oral Cancer: A Comprehensive Guide. Journal of Pharmacy and Bioallied Sciences. 2024; 16(5): S4239-S4241.
[21] Natarajan PM. Computational Studies on Recent Congeners of Fluoroquinolones and Nitroimidazoles for Their Use in Periodontal Therapy. Journal of Pharmacy and Bioallied Sciences. 2024; 16(5): S4731-S4740.
[22] Natarajan PM, Bhuminathan S, Rajan R, Bindu K, Loganathan K, Veerakumar R. The Crucial Role of Smoking Cessation in Preventing Oral Cancer. Journal of Pharmacy and Bioallied Sciences. 2024; 16(5): S4245-S4247.
[23] Natarajan PM, Bhuminathan S, Leela B, Bindu K, Loganathan K, Ramachandran V. Smoking and its Role in Oral Cancer. Journal of Pharmacy and Bioallied Sciences 16(5): S4242-S4244.
[24] Vidhyarekha U, Natarajan PM, Bhuminathan S, Sabarinathan J, Suba R, Vijayalakshmi P. Role of artificial intelligence in Oral Cancer. Advances in Public Health. 2024. 2024: 3664408.
[25] Ganesan A, Kumar NG, Natarajan PM, Gauthaman J. Automated classification of elongated styloid processes using deep learning models-an artificial intelligence diagnostics. Frontiers in Oral Health. 2025; 5: 1424840.
[26] Umapathy VR, Natarajan PM, Swamikannu B. Regenerative Strategies in Dentistry: Harnessing Stem Cells, Biomaterials and Bioactive Materials for Tissue Repair. Biomolecules. 2025; 15: 546.
[27] Guan T, Gong J, Lin J, Palanisamy CP, Jinjin Pei J, El-Aty AMA. Machine learning-driven multimodal optimization of selenium biotransformation and flavor profiling in fermented apple–Yacon functional beverages. Innovative Food Science & Emerging Technologies. 2025; 105: 104198.
[28] Natarajan SR, Krishnamoorthy R, Alshuniaber MA, Alsulami TS, Gatasheh MK, Rajagopal P, Palanisamy CP, Govindan R, Veeraraghavan VP, Jayaraman S. ABCE1 facilitates tumour progression via aerobic glycolysis and inhibits cell death in human colorectal cancer cells through the p53 signalling pathway. Scientific Reports. 2025; 15: 24674.
[29] Huang Y, Guo H, Liu Y, Jin W, Palanisamy CP, Pei J, Oz F, El-Aty AMA. Effects of Natural Polysaccharides on the Gut Microbiota Related to Human Metabolic Health. Molecular Nutrition & Food Research. 2025; 69:e202400792.
[30] Poornima K, Meenakshi K.C, Manikandan V.R, Shankari G, Prabhu D, Rathi M.A, Palanisamy CP, Balaji

R, Gopalakrishnan V.K. Exploring the anticancer potential of Jerantinine A from *Tabernaemontana coronaria* against prostate, breast, and ovarian cancers: A computational approach. *Journal of Complementary and Integrative Medicine*, 2025 22(2): 363–372.

[31] Palanisamy CP, Poompradub S, Sansanaphongpricha K, Jayaraman S, Subramani K. Faridah Sonsudin gGreen synthesis of Nigella sativa-mediated silver nanoparticles for enhanced antibacterial activity and wound healing: Mechanistic insights and biomedical applications. Environmental Nanotechnology, Monitoring & Management. 2025; 24: 101085.

[32] Surendran N, Raju MV, Chandrasekaran MK, Ahalliya RM, Palanisamy CP, Chandrasekaran G, Kanniappan GV. Physicochemical characterization of starch from Maranta arundinacea L.(arrowroot) rhizomes and its inhibition of COX-2: In vivo validation. Bioactive Carbohydrates and Dietary Fibre. 2025; 33: 100465.

[33] Kannappan P, Chandrasekaran MK, Raju MV, Gopalakrishnan S, Dhamodharan P, Ahalliya RM, Palanisamy CP, Raju B, Kanniappan GV. Exploring the anticancer potential of Jerantinine A from Tabernaemontana coronaria against prostate, breast, and ovarian cancers: a computational approach. Journal of Complementary and Integrative Medicine. 2025; 22(02): 363-372.

[34] Pei J, Kumarasamy RV, Jayaraman S, Kanniappan GV, Long Q, Palanisamy CP. Quercetin-functionalized nanomaterials: Innovative therapeutic avenues for Alzheimer's disease management. Ageing Research Reviews. 2025; 104: 102665.

[35] Jayaraman S, Prasad M, Natarajan SR, Krishnamoorthy R, Alshuniaber MA, Gatasheh MK, Veeraraghavan VP, Rajagopal P, Palanisamy CP. Molecular mechanisms underlying the effects of beta-sitosterol on TGF-β1/Nrf2/SIRT1/p53-mediated signaling in the kidney of a high-fat diet and sucrose-induced type-2 diabetic rat. Chemico-Biological Interactions. 2025; 411: 111443.

[36] Huang Y, Guo H, Liu Y, Jin W, Palanisamy CP, Pei J, Oz F, El-Aty AMA. Effects of Natural Polysaccharides on the Gut Microbiota Related to Human Metabolic Health. Molecular Nutrition & Food Research. 2025; e202400792.

[37] Prabhakaran P, Palanisamy CP, Shanmugam A, Damodharan P, Swaminathan H, Devaraj D, Ahalliya RM, Kanniappan GV. Isolation, structural characterization, and molecular docking studies on the bioactive compound from n-Hexane extract of Emilia sonchifolia (L.) DC against the pancreatic cancer target Aurora 2 Kinase. Journal of Complementary and Integrative Medicine. 2024; 22(1): 0290.

[38] Jiang H, Kumarasamy RV, Pei J, Raju K, Kanniappan GV, Palanisamy CP. Integrating engineered nanomaterials with extracellular vesicles: Advancing targeted drug delivery and biomedical applications. Frontiers in Nanotechnology. 2024; 6: 1513683.

[39] Guo H, Liu Y, Wan T, Song D, Palanisamy CP, Geng J, Pei J, Özmen S, El-Aty AMA. Toward personalized cancer management: Role of precision nutrition–diet interventions. Journal of Functional Foods. 2024; 123: 106584.

[40] Natarajan SR, Krishnamoorthy R, Alshuniaber MA, Al-Anazi KM, Farah MA, Rajagopal P, Palanisamy CP, Veeraraghavan VP, Jayaraman S. Identification of FOXM1 as a novel protein biomarker and therapeutic target for colorectal cancer progression: Evidence from immune infiltration and bioinformatic analyses. International Journal of Biological Macromolecules. 282 (Part 4): 137201.

[41] Ganesan A, Kumar NG, Natarajan PM. Solanum trilobatum leaf extract-derived silver nanoparticles downregulate the PI3K/AKT/mTOR signaling pathway and attenuate oral squamous cell carcinoma cell proliferation. Journal of Herbmed Pharmacology. 2024; 13(2): 300-307.

[42] Perumal MKK, Renuka RR, Subbiah SK, Natarajan PM. Artificial intelligence-driven clinical decision support systems for early detection and precision therapy in oral cancer: a mini review. Frontiers in Oral Health. 2025; 6: 1592428.

[43] Ramesh E, Ganesan A, Lakshmi KC, Natarajan PM. Artificial intelligence-based diagnosis of oral leukoplakia using deep convolutional neural networks Xception and MobileNet-v2. Frontiers in Oral Health. 2025; 6: 1414524.

[44] Ganesan A, Kumar NG, Natarajan PM. Anticancer activity of silver nanoparticles synthesized from aqueous leaf extract of Solanum trilobatum (Purple fruit pea eggplant) on human oral cancer cells. Journal of Herbmed Pharmacololgy. 2024; 13(2): 260-268.

[45] Umapathy V, Dhanavel A, Kesavan R, Natarajan PM, Bhuminathan S, Vijayalakshmi P. Anticancer Potential of the Principal Constituent of Piper nigrum, Piperine: A Comprehensive Review. Cureus. 2024; 16(2): e54425.

[46] Umapathy VR, Swamikannu B, Natarajan PM, Devi R, Nandini MS, Vimalarani, Vijayalakshmi P. In Silico Molecular Docking of Ocimum sanctum Phytochemicals: Targeting Key Biomarkers in Oral Cancer. Journal of Pharmacy and Bioallied Sciences. 2024; 16(5): S4792-S4799.

[47] Swamikannu B, Umapathy VR, Natarajan PM, Nandini MS, Stylin AGSQ, Vimalarani V, Rajinikanth S. Unlocking the Therapeutic Benefits of Artemisia Annua: A Comprehensive Overview of its Medicinal Properties. Journal of Pharmacy and Bioallied Sciences. 2024; 16(5): S4248-S4253.

[48] Yadalam PK, Arumuganainar D, Natarajan PM, Ardila CM. Artificial intelligence-powered prediction of AIM-2 inflammasome sequences using transformers and graph attention networks in periodontal inflammation. Scientific Reports. 2025; 15: 8733.

[49] Yadalam PK, Chatterjee S, Natarajan PM, Ardila CM. Comparison of light gradient boosting and logistic r egression for interactomic hub genes in Porphyromonas gingivalis and Fusobacterium nucleatum-induced periodontitis with Alzheimer's disease. Frontiers in Oral Health. 2025; 6:1463458.
[50] Yadalam PK, Natarajan PM, Ardila CM. Variational graph autoencoder for reconstructed transcriptomic data associated with NLRP3 mediated pyroptosis in periodontitis. Scientific Reports. 2025; 15: 1962.
[51] Daniel Raja FS, Abraham L, Rangasamy K, Saikia K, Rathankumar AK, Mironescu M, Mironescu I, Palanisamy CP, Kanniappan GV. Next-Generation Microbiome Therapeutics: Psychobiotics and Fecal Microbiota Transplants (FMT) for Mental Health Treatment. Frontiers in Cellular and Infection Microbiology. 2026; 16: 1719357.
[52] Dharmaprakash S, Gunasekaran VP, Sivaramakrishnan R, Kanniappan GV, Jayaraman S, Mironescu M, Rajabathar JR, Mironescu ID, Palanisamy CP. Marine macroalgae-mediated ultrasonic-assisted green synthesis of CuO nanoparticles embedded in starch/PVA electrospun nanoscaffolds for in vitro α-amylase and α-glucosidase inhibitory activity. Scientific Reports. 2026.
[53] Surendran N, Chandrasekaran G, Raju MV, Chandrasekaran MK, Ahalliya RM, Palanisamy CP, Kanniappan GV, Arcot R, Alharbi NS, Thiruvengadam M. Anti-inflammatory potential of ethanolic extract of Maranta arundinacea L.: Insights from COX-2 modulation and oxidative stress analysis. South African Journal of Botany. 2026; 195: 142-151.
[54] Pei J, Senthilkumar MV, Hessini K, Subramaniyam S, Sivaramakrishnan R, Kanniappan GV, Jayaraman S, Palanisamy CP. Green fabrication of starch/PVA/CuO nanoscaffolds using marine macroalgae extract for enhanced anti-inflammatory activity. Sustainable Chemistry and Pharmacy. 2026; 51: 102397.
[55] Balasubramanian V, Loganathan L, Muthuswamy K, Viswanathan TM, Raju MV, Chandrasekaran MK, Ahalliya RM, Poorasamy J, Palanisamy CP, Dominic S, Kanniappan GV. Anticancer therapeutic efficacy of PEGylated β-galactosidase from Aspergillus terreus in DMBA-induced breast cancer: Toxicological, molecular and histopathological evaluation in Wistar rats. International Journal of Biological Macromolecules. 2026; 360: 151856.
[56] Jayaraman S, Eswaran A, Rajagopal P, Palanisamy CP, Veerakumar P, Veeraraghavan VP, Sirasanagandla SR. Neuroendocrine-associated epigenetic factors in cellular senescence: mechanisms and therapeutic implications. Biogerontology. 2026; 27(2): 64.
[57] Ponnusamy B, Rajagopal P, Palanisamy CP, Veeraraghavan VP, Jayaraman S. Mechanistic Exploration of the anticancer activity of Justicia adhatoda Plant Leaf Ethanolic Extract against Colon Cancer Cells: An in silico and in vitro Approach. Asian Pacific Journal of Cancer Prevention. 2026; 27(3): 1069-1080.
[58] Pei J, Saran VS, Sivaramakrishnan R, Kanniappan GV, Pandurangan V, Jayaraman S, Dhayalan VK, Mironescu M, Mironescu ID, Palanisamy CP. Ultrasonic-assisted, Sargassum ilicifolium (brown marine macroalgae)-mediated biogenic synthesis of CuO nanoparticles incorporated in starch/PVA electrospun nanoscaffolds: In vitro safety and antioxidant efficacy assessment. Bioorganic Chemistry. 2026; 173: 109679.
[59] Raj MAPA, Subramaniyam S, Kanniappan GV, Jayaraman S, Palanisamy CP. Sustainable fabrication of starch/PVA/CuO electrospun nanoscaffolds from Turbinaria ornata (marine macroalgae) extract: Physicochemical characterization and antidiabetic evaluation. Kuwait Journal of Science. 2026; 53(2): 100545.
[60] Pei J, Ganesh NS, Subramaniyam S, Sivaramakrishnan R, Kanniappan GV, Jayaraman S, Palanisamy CP. Sustainable fabrication of starch/PVA/CuO electrospun nanoscaffolds from Padina tetrastromatica (Brown macroalgae) extract: Physicochemical characterization and antidiabetic assessment. Sustainable Chemistry One World. 2026; 9: 100195.
[61] Sakthiraj A, Sivaramakrishnan R, Subramaniyam S, Kanniappan GV, Pandurangan V, Jayaraman S, Dhayalan VK, Mironescu M, Mironescu ID, Palanisamy CP. Starch/PVA electrospun nanoscaffolds loaded with ultrasonic-assisted green-synthesis of CuO nanoparticles from marine macroalgae (Gracilaria corticata) extract: Cytotoxicity and antioxidant analysis. Chemical Physics Impact. 2026; 12: 101018.
[62] Raju M, Chandrasekaran MK, Loganathan L, Ahalliya RM, Mironescu M, Mironescu ID, Palanisamy CP, Kanniappan GV. Lipid remodeling and ferroptosis in phosphatidylcholine-mediated tumor–stroma crosstalk. Frontiers in Molecular Biosciences. 2026; 13: 1742305.
[63] Kunamalla R, Panagal M, Palanisamy CP. Biogenic synthesis and fabrication of starch/PVA/CuO electrospun nanoscaffolds from Sargassum ilicifolium (brown marine macroalgae) extract for anticancer activity on HT-29 and MCF-7 cancer cells. Biocatalysis and Agricultural Biotechnology. 2026; 72: 103923.
[64] Pei J, Govindaraj H, Sivaramakrishnan R, Kanniappan GV, Pandurangan V, Dhayalan VK, Mironescu M, Mironescu ID, Jayaraman S, Palanisamy PC. Sustainable fabrication of biopolymer-based (starch/PVA) nanoscaffolds loaded with green-synthesized CuO nanoparticles from Sargassum wightii (marine macroalgae): Cytocompatibility and antioxidant activity. Biomaterials Advances. 2026; 182: 214660.
[65] Pei J, Perumal NC, Meng P, Long Q, Palanisamy CP. Extracellular vesicle-based biosensors for Alzheimer's disease: A new frontier in precision diagnostics. Ageing Research Reviews. 2026; 113: 102904.
[66] Shree P, Sivaramakrishnan R, Kanniappan GV, Pandurangan V, Jayaraman S, Dhayalan VK, Mironescu M, Mironescu ID, Palanisamy CP. Antioxidant and biocompatible CuO-starch/PVA nanoscaffolds via ultrasonic green synthesis using Turbinaria conoides (brown marine macroalgae). Medicine in Drug

Discovery. 2025; 28: 100238.
[67] Gong J, Lin J, Guan T, Pei J, Palanisamy CP, El-AtyFrom AMA. selenium tolerance to nanoplastic antagonism: Comprehensive characterization of L. casei SNUT1 and its extracellular vesicle–nanoselenium complex. Food Bioscience. 2025; 74: 107749.
[68] Poochi SP, Sundarraj R, Raju MV, Chandrasekaran MK, Ahalliya RM, Palanisamy CP, Kanniappan GV, Kondapavuluri BK, Thiruvengadam M. Harnessing Nature: Computational and Experimental Insights Into *Ipomoea obscura* Metabolites for Bladder Cancer Therapy. Chemistry and Biodiversity. 2025; 0: e00909.
[69] Dugganaboyana GK, Kannankumar MKG, Shivaramakrishna S, Raju MV, Chandrasekaran MK, Ahalliya RM, Panneerselvam N, Palanisamy CP, Kanniappan GV. Phytochemical insights, antioxidant activity and therapeutic potential of Cassia senna against prostate cancer in Wistar albino rats. Discover Applied Sciences. 2025; 7:1206.
[70] Natarajan SR, Krishnamoorthy R, Alshuniaber MA, Gatasheh MK, Rajagopal P, Veeraraghavan VP, Palanisamy CP, Jayaraman S. KDM1A Facilitates Oncogenic Potential in Colorectal Cancer Progression Through the Activation of AXIN/GSK3β/β-Catenin Signaling Pathways: Evidence From Integrated Transcriptomics and In Vitro Studies. The Journal of Gene Medicine. 2025; 27(11): e70053.
[71] Prasad M, Jayaraman S, Natarajan SR, Veeraraghavan VP, Krishnamoorthy R, Gatasheh MK, Palanisamy CP, Elrobh M. Piperine modulates IR/Akt/GLUT4 pathways to mitigate insulin resistance: Evidence from animal and computational studies. International Journal of Biological Macromolecules. 2023; 253: 127242.
[72] Palanisamy CP, Pei JJ, Phaniendra A, Venkata AAN, Jayaraman S, Veeraragahavan VP, Sridevi G, Roy JR, Janaki CS, Thalamati D, Mironescu M, Luo Q, Chai Y, Long Q. New Strategy of Neurodegenerative Disease Treatment with Extracellular Vesicles (EVs) Derived from Mesenchymal Stem Cells (MSCs). *Theranostics*. 2023; 13(12):4138-4165. doi:10.7150/thno.83066.
[73] Palanisamy CP, Phaniendra A, Jayaraman S, Poompradub S. *Nigella sativa* L. seed extracts promotes wound healing progress by activating VEGF and PDGF signalling pathways: *An in vitro* and *in silico* study. *F1000 Research*. 2023; 12: 436.
[74] Pei JJ, Palanisamy CP, Phaniendra A, Venkata AAN, Natarajan PM, Umapathy VR, Swamikannu B, Jayaraman S, Rajagopal P, Poompradub S. A comprehensive review on bio-based materials for chronic diabetic wounds. *Molecules*. 2022; 28(2), 604.